

Parádsasvárite, a new member of the malachite-rosasite group from Parádsasvár, Mátra Mountains, Hungary

Béla Fehér · Sándor Szakáll · Norbert Zajzon ·
Judith Mihály

Received: 22 July 2014 / Accepted: 6 February 2015 / Published online: 5 March 2015
© Springer-Verlag Wien 2015

Abstract Parádsasvárite (IMA No. 2012-077) was found in the Nagy-Lápafő area, Parádsasvár, Mátra Mountains, Hungary. It forms pale beige, globular aggregates up to 0.2 mm in diameter on calcite. Associated secondary minerals are smithsonite, hemimorphite, hydrozincite, aurichalcite and rosasite. The mineral was formed as an alteration product of sphalerite and chalcopyrite in a carbonate-rich environment. Parádsasvárite is translucent with a weakly vitreous, dull or silky lustre and white streak. Its Mohs hardness is about 2–3, cleavage and parting were not observed. It is brittle; the fracture is finely fibrous. Average of nine electron-microprobe analyses gave ZnO 58.08, CuO 12.60, PbO 1.27, CO₂ (calc.) 19.50, H₂O (calc.) 7.94, total 99.39 wt.%, corresponding to the empirical formula (Zn_{0.62}Cu_{0.36}Pb_{0.01})_{Σ0.99}Zn_{1.00}(CO₃)(OH)₂. The seven strongest lines in the X-ray powder diffraction pattern are [*d*_{hkl} in Å (*I*_{obs} %, *hkl*)] 6.054 (67, 200), 5.085 (100, 210), 3.703 (87, 310 and 220), 3.021 (25, 400 and 130), 2.971 (25, –211 and 001), 2.603 (62, –221) and 2.539 (36, 420). According to its X-ray powder diffraction data and chemical formula, parádsasvárite belongs to the malachite-rosasite group and it is isostructural with rosasite. It is monoclinic, space group *P*2₁/*a*, *a* = 12.92(1),

b = 9.372(7), *c* = 3.159(4) Å, β = 110.4(1)°, *V* = 358.5(5) Å³, *Z* = 4.

Introduction

Rosasite, the zinc-rich member of the malachite-rosasite group of minerals, has been known for a long time (Lovisato 1908). In the literature its formula is given as (Cu, Zn)₂(CO₃)(OH)₂ (see e.g., Anthony et al. 2003); this formula indicates a disordered distribution of Cu and Zn, with the former as dominant cation. The zinc-dominant phase was described by Strunz (1959) from Tsumeb, Namibia, and named zincrosasite. Its description is very short, since it consists of six sentences and no figures or tables are presented. The author did not produce a chemical analysis or empirical formula for the mineral; in fact, he indicated the Zn:Cu ratio only, which is equal to 58.60:51.94 corresponding to a chemical formula (Zn_{1.06}Cu_{0.94})(CO₃)(OH)₂. Present status of zincrosasite in the most recent IMA list of mineral species (IMA 2014) is Q (questionable), with chemical formula (Zn, Cu)₂(CO₃)(OH)₂.

To date, several occurrences of zincrosasite have been described worldwide and the Mindat.org database lists 24 localities for it (<http://www.mindat.org/min-4414.html>). Unfortunately, the available chemical analyses for zincrosasite are a very few. Pauliš et al. (2005) give the formula (Zn_{1.15}Cu_{0.85})(CO₃)(OH)₂ for the sample of the mineral found at Herlíkovice in the Czech Republic. The sample of zincrosasite with the highest zinc content was described by Fehér et al. (2008) from Rudabánya in Hungary with chemical formula (Zn_{1.52}Cu_{0.47}Fe_{0.01})(CO₃)(OH)₂.

Following Perchiazzi and Merlino (2006), two distinct structural types exist in the malachite-rosasite group, namely a malachite structure type (Zigan et al. 1977) and a rosasite structure type (Perchiazzi 2006). In both of the above structure

Editorial handling: A. Beran

B. Fehér (✉)
Department of Mineralogy, Herman Ottó Museum, Kossuth u. 13,
3525 Miskolc, Hungary
e-mail: feherbela@upcmail.hu

S. Szakáll · N. Zajzon
Department of Mineralogy and Petrology, University of Miskolc,
3515 Miskolc-Egyetemváros, Hungary

J. Mihály
Institute of Materials and Environmental Chemistry, Research Center
for Natural Sciences, Hungarian Academy of Sciences, Pusztaszeri út
59-67, 1025 Budapest, Hungary

types, two hexacoordinated cation sites, named *Me1* and *Me2*, exist. The former displays a Jahn-Teller distorted 4 + 2 coordination, quite common in copper oxysalts (Eby and Hawthorne 1993). *Me2* site displays a more regular octahedral coordination. Several mineral species are known in this group, defined by the dominant cation on the *Me* sites and by their structural type (see Perchiazzi and Merlino 2006). In this sense, zincrosasite does not define a distinct mineral species, because the dominant cations are copper in *Me1* and zinc in *Me2*, which is the same in the case of rosasite. The difference

between rosasite and zincrosasite is the total cation content (*Me1* + *Me2*), which is not relevant in the nomenclature.

Here we describe the new mineral parádsasvárite, which represents the Zn-dominant end-member of the malachite-rosasite group, where zinc is the dominant cation in both *Me1* and *Me2* sites. The mineral was approved by the Commission on New Minerals, Nomenclature and Classification of the International Mineralogical Association (IMA CNMNC) under IMA no. 2012-077. The holotype material is deposited in the collection of the Herman Ottó

Fig. 1 Geological map of the surroundings of the type locality of parádsasvárite (after Rónai and Pelikán 2005). Legend: 1: fluvial sediments (Holocene); 2: Kékes Andesite Formation (Miocene, Badenian-Sarmatian); 3: Nagyhársas Andesite Formation (Miocene, Badenian); 4: Tar Dacite Tuff Formation (Miocene, Carpathian); 5: Hasznos Andesite Formation (Miocene, Carpathian); 6: Fót Formation (Miocene, Carpathian); 7: Garáb Schlier Formation (Miocene, Carpathian); 8: Gyulakeszi Rhyolite Tuff Formation (Miocene, Ottnangian); 9: Zagyvapálfalva Formation (Miocene, Eggenburgian); 10: Pétervására Sandstone Formation (Miocene, Egerian-Eggenburgian)

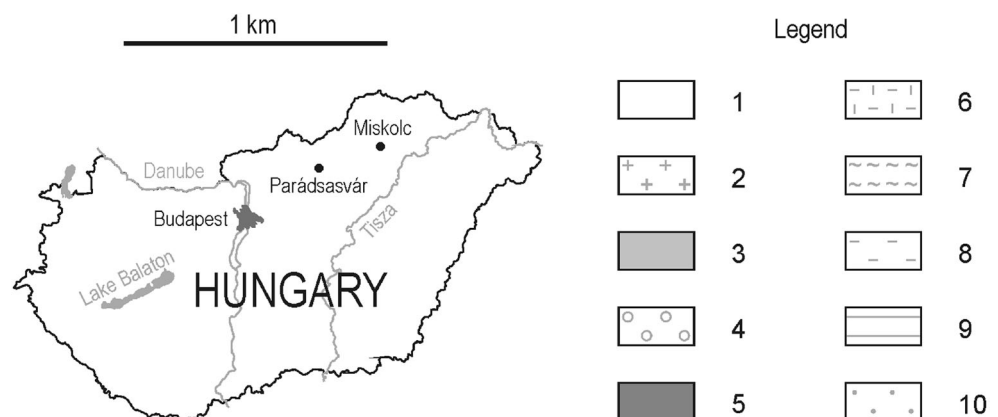
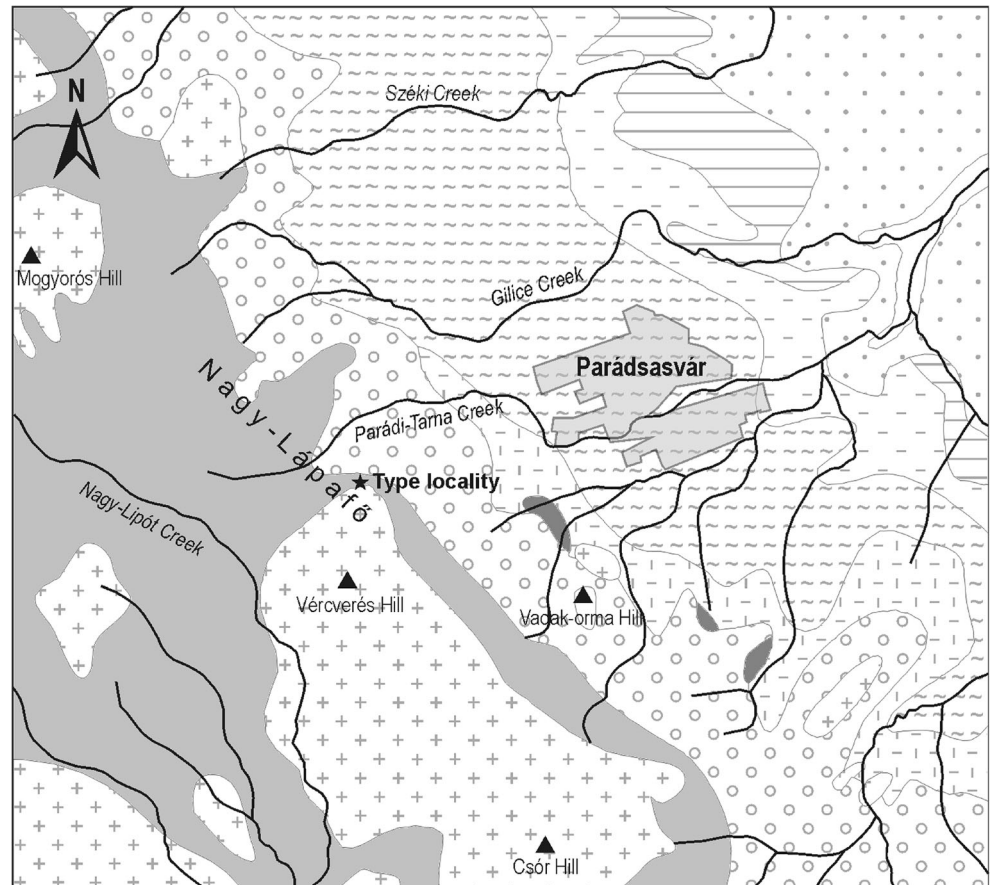




Fig. 2 Globular parásasváríte aggregates on calcite from Parádsasvár. Short edge of the picture: 0.8 mm. Photo courtesy of László Tóth

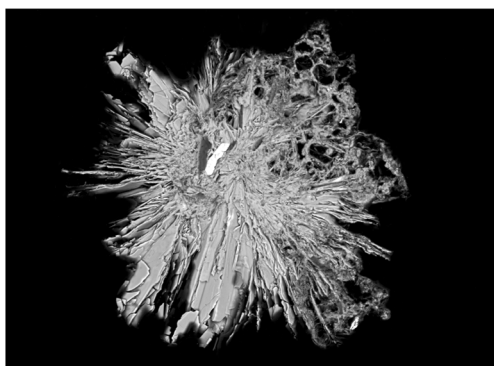
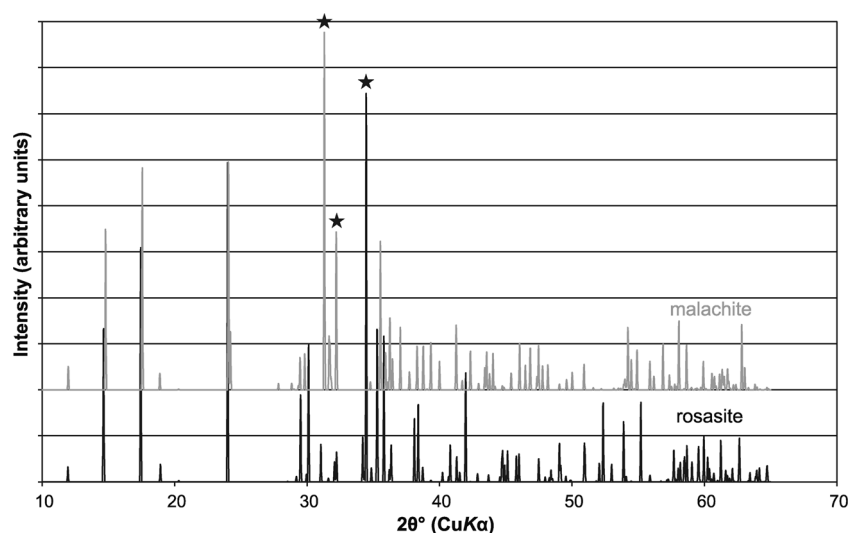


Fig. 3 Section of a globular parásasváríte aggregate consisting of bladed crystals; BSE-SEM image. Long edge of the picture: 380 μm

Fig. 4 Calculated X-ray powder diffraction patterns for malachite and rosasite. Atomic coordinates used in the calculation are from Zigan et al. (1977) for malachite and from Perchiazzi (2006) for rosasite. Diagnostic reflections are indicated by asterisks



Museum, Miskolc, Hungary, under catalogue number 2012.23. Parádsasváríte was named after the type locality Parádsasvár, in the Mátra Mountains of Hungary.

Geologic frame

Parásasváríte was found in a near-surface epithermal ore mineralization in the Nagy-Lápafő area, Parádsasvár, Mátra Mountains, Hungary (Fig. 1) ($47^{\circ}54'26.50''\text{N}$, $19^{\circ}57'9.68''\text{E}$). This ore mineralization is connected with the Middle Miocene andesitic volcanism (Nagyhársas Andesite Formation) of the Mátra Mountains. During the construction of a forest road, carbonate veins up to a few dm in thickness were exposed in the andesite, and these were found to contain disseminated sulphide minerals. Secondary minerals, formed by alteration of the sulphides, can be found in small cavities of the veins.

The main mineral of the carbonate veins, which are located in argillized and pyritized andesite, is calcite. The most abundant sulphide mineral is sphalerite, but several other sulphides were also found here in lesser quantities: galena, pyrite, chalcocopyrite, marcasite, hawleyite/greenockite, and tetrahedrite. Beside calcite, the other gangue minerals in the veins are fluorite, palygorskite, quartz, dolomite, and anatase. At the contact of the andesite and carbonate veins there are clay minerals, such as montmorillonite, illite and kaolinite, as well as gibbsite; these were observed as hydrothermal alteration products (Kiss 1960, 1964; Koch 1966). To date, the following secondary minerals have been detected, and here they are given in their order of decreasing abundance: smithsonite, hydrozincite, hemimorphite, aurichalcite, rosasite, malachite, chalcophanite, azurite, cerussite, anglesite, devilline, and linarite.

Table 1 X-ray powder diffraction data for parádsasvárite

I_{rel} (%)	d_{meas} (Å)	d_{calc} (Å)	h	k	l
11	7.431	7.411	1	1	0
67	6.054	6.054	2	0	0
100	5.085	5.085	2	1	0
14	4.678	4.686	0	2	0
87	3.703	3.707	3	1	0
		3.706	2	2	0
25	3.021	3.027	4	0	0
		3.025	1	3	0
25	2.971	2.964	-2	1	1
		2.960	0	0	1
10	2.880	2.881	4	1	0
7	2.773	2.776	2	3	0
62	2.603	2.599	-2	2	1
36	2.539	2.543	4	2	0
23	2.498	2.503	0	2	1
15	2.478	2.480	-3	2	1
		2.470	3	3	0
20	2.346	2.355	2	0	1
		2.345	5	1	0
		2.343	0	4	0
5	2.212	2.209	-2	3	1
19	2.150	2.151	5	2	0
		2.149	0	3	1
12	2.016	2.019	3	1	1
5	1.975	1.983	-6	1	1
		1.973	6	1	0
4	1.910	1.914	5	3	0
6	1.852	1.858	-5	3	1
7	1.785	1.791	2	5	0
		1.789	4	1	1
8	1.748	1.747	-4	4	1
6	1.699	1.702	-6	3	1
7	1.656	1.661	2	4	1
7	1.589	1.594	5	1	1
10	1.568	1.570	-2	0	2
9	1.544	1.541	-4	1	2
5	1.510	1.512	2	6	0
4	1.479	1.482	5	5	0
3	1.410	1.412	0	2	2
		1.410	-9	1	1
4	1.385	1.388	4	6	0

Sample material and experimental

Parádsasvárite occurs as pale beige, globular aggregates up to 0.2 mm in diameter and consists of bladed crystals in a radial arrangement on calcite (Figs. 2 and 3). The individual bladed crystals are up to $80 \times 5 \mu\text{m}$. The colour on the surface

Table 2 Electron microprobe data for parádsasvárite

Constituent	Mean wt.% ($n = 9$)	Range in wt.%	σ
ZnO	58.08	55.00–63.08	2.70
CuO	12.60	8.76–15.18	2.17
PbO	1.27	0.55–1.65	0.29
CO ₂ ^a	19.50		
H ₂ O ^a	7.94		
Total	99.39		

^a Calculated from the stoichiometry

of the aggregates is pale beige, while sections of the globular aggregates are white, sometimes with a weak bluish tint. Its lustre is weakly vitreous or dull on the surface of the aggregates and silky in cross-sections. The streak is white and the Mohs hardness is about 2–3. The mineral does not show any discernible fluorescence under long-, or short-wave ultraviolet radiation. Tenacity is rather brittle. Cleavage and parting were not observed. Fracture of the aggregates is finely fibrous.

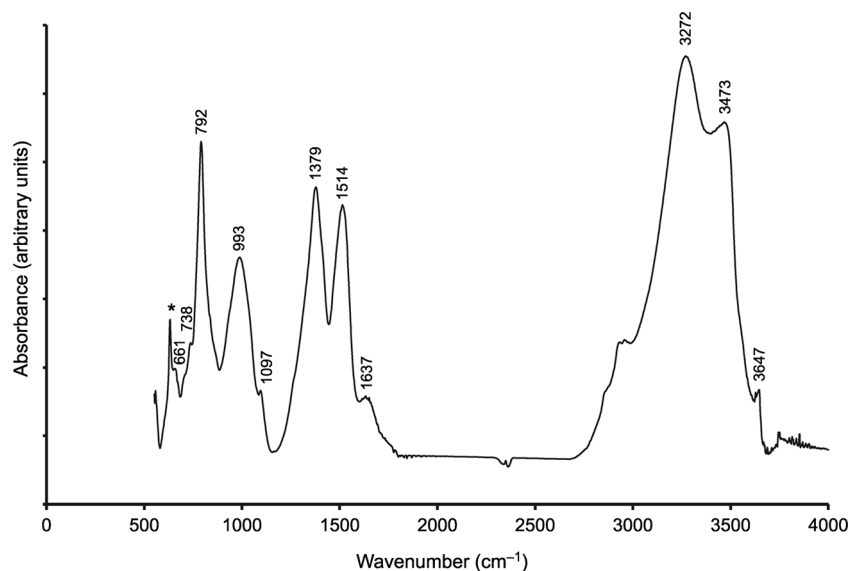
Density could not be measured directly due to the very limited amount of type material available as well as the fact that the expected density $>4.1 \text{ g/cm}^3$. Moreover, an accurate value of measured density cannot be expected because of the porous nature of the aggregates (see Fig. 3). Parádsasvárite has a calculated density of 4.175 g/cm^3 , as determined using the empirical chemical formula.

Optical properties could not be determined (except for pleochroism) due to the very small sizes of the crystals. The pleochroism is very weak and is colourless to very pale green. Mean refractive index calculated from the Gladstone-Dale equation (see Mandarino 1981) using the measured composition and the calculated density is $n = 1.764$.

Because of its microcrystalline habit, single-crystal X-ray studies could not be carried out on parádsasvárite. X-ray powder diffraction data were collected using Ni-filtered $\text{CuK}\alpha$ radiation and a 114.6 mm diameter Gandolfi camera. Operating conditions were as follows: accelerating voltage 40 kV, tube current 40 mA, and exposition time 47 h. Synthetic silicon powder (NIST SRM 640) was used as the internal standard for film shrinkage. The Gandolfi film was scanned using a UMAX PowerLook 3000 scanner with a resolution of 3000 dpi; it was processed by QSpec software (Zelensky et al. 2009).

Nine quantitative point analyses were performed using a JEOL JXA-8600 electron microprobe operated in wavelength-dispersive mode. Operating conditions were as follows: accelerating voltage 20 kV, probe current 20 nA, a final beam diameter of $10 \mu\text{m}$, the peak count-times were 20 s and the background count-times were 10 s. The standards employed were: pure Zn (Zn), pure Cu (Cu) and PbS (Pb). Raw intensity data were corrected using a PAP matrix correction (Pouchou and Pichoir 1984).

Fig. 5 The IR spectrum of parásasváríte (* = sapphire head)



An aggregate of parásasváríte was investigated using a Varian 2000 FTIR spectrometer with a single reflection diamond ATR accessory and an MCT detector with a 4 cm^{-1} resolution, and 128 scans. The IR spectrum is limited by the cut-off point at 550 cm^{-1} of the broad band MCT detector. The region $2000\text{--}2300\text{ cm}^{-1}$ cannot be evaluated due to the strong absorption of the diamond ATR cell.

Results and discussion

X-ray crystallography

Apart from malachite (Zigan et al. 1977) and rosasite (Roberts et al. 1986), single-crystal studies are missing for the members of the malachite-rosasite group; this is mainly because of their microcrystalline, fibrous habit. The symmetry and cell parameters of all the other members (see Table 3) were mainly deduced from powder pattern indexing (Perchiazzi 2006).

As reported by Perchiazzi (2006), two structure types can be distinguished in the malachite-rosasite group – namely, a malachite-like and a rosasite-like structure. The difference between them was treated in detail by Perchiazzi and Merlino (2006). According to the structural investigations performed on the members of the group, only malachite belongs to the malachite-type structure. All the other members which have so far undergone crystal structure determination (rosasite, mcguinnessite – Perchiazzi 2006; glaukosphaerite, pokrovskite – Perchiazzi and Merlino 2006; chukanovite – Pekov et al. 2007) have a rosasite-type structure.

Although malachite- and rosasite-type structures have very similar X-ray powder diffraction patterns, they can be distinguished clearly (on the basis of their respective peak intensities) in the region of $30\text{--}40^\circ 2\theta$ ($\text{CuK}\alpha$ radiation). As shown in Fig. 4, there are two strong reflections at 31.3° (100 %,

2.856 \AA) and 32.2° (43 %, 2.778 \AA) on the calculated pattern of malachite (relative intensities and d -values are in brackets), while on the same positions only low intensity peaks (9 and 8 %, respectively) can be found in the case of rosasite. Conversely, the strong reflection on the rosasite pattern at 34.46° (100 %, 2.600 \AA) has no counterpart on the malachite pattern.

According to its X-ray powder diffraction pattern (Table 1), parásasváríte is structurally analogous to rosasite. Least-squares refinement of the powder diffraction data using the program UnitCell (Holland and Redfern 1997) and 31 indexed lines leads to $a = 12.92(1)$, $b = 9.372(7)$, $c = 3.159(4)\text{ \AA}$, $\beta = 110.4(1)^\circ$, $V = 358.5(5)\text{ \AA}^3$, and $Z = 4$. Unit cell parameters and the cell volume of parásasváríte are very close to that reported for rosasite by Perchiazzi (2006) (see Table 3).

The crystal structure data of rosasite determined by Perchiazzi (2006) was used for calculating the X-ray powder pattern of parásasváríte, where the $Me1$ site is occupied by $0.63\text{Zn} + 0.36\text{Cu} + 0.01\text{Pb}$ and the $Me2$ site is occupied entirely by Zn. For the calculation the PowderCell 2.4 software (Kraus and Nolze 1996) was applied.

Chemical composition

In Table 2 the mean values and ranges of chemical analyses are listed alongside the standard deviations. H_2O and CO_2 were not determined because of the very limited amount of type material available. The presence of OH and CO_3 groups was confirmed by FTIR spectroscopy. H_2O and CO_2 contents were calculated from the stoichiometry. Due to the lack of data concerning the crystal structure of parásasváríte, the cation distribution between $Me1$ and $Me2$ sites is unknown. In order to give a structural formula for parásasváríte, a full occupancy by zinc for the $Me2$ position was assumed. This is because zinc tends to occupy the smaller, more regular $Me2$ octahedron (Perchiazzi 2006). For the $Me1$ site a mixed occupancy $\text{Zn}_{0.62}\text{Cu}_{0.36}\text{Pb}_{0.01}$ was

Table 3 Members of the malachite-rosasite group. Cations dominating in *Me1* and *Me2* sites are reported for each phase

Name	<i>Me1</i>	<i>Me2</i>	Space group	Lattice parameters	Reference
Malachite	Cu	Cu	$P2_1/a$	a = 9.502 b = 11.974 c = 3.240 Å β = 98.75° V = 364.34 Å ³	Zigan et al. (1977)
Rosasite	Cu	Zn	$P2_1/a$	a = 12.8976(3) b = 9.3705(1) c = 3.1623(1) Å β = 110.262(3)° V = 358.54(2) Å ³	Perchiazzi (2006)
Parádsasvárite	Zn	Zn	$P2_1/a$	a = 12.92(1) b = 9.372(7) c = 3.159(4) Å β = 110.4(1)° V = 358.5(5) Å ³	This work
Mcguinnessite	Cu	Mg	$P2_1/a$	a = 12.9181(4) b = 9.3923(2) c = 3.1622(1) Å β = 111.233(3)° V = 357.63(2) Å ³	Perchiazzi (2006)
Glaukosphaerite	Cu	Ni	$P2_1/a$	a = 12.0613(4) b = 9.3653(4) c = 3.1361(1) Å β = 98.085(5)° V = 350.73 Å ³	Perchiazzi and Merlino (2006)
Kolwezite	Cu	Co	$P-1$ or $P1$	a = 9.50 b = 12.15 c = 3.189 Å α = 93.32° β = 90.74° γ = 91.47° V = 367.31 Å ³	Deliens and Piret (1980)
Nullaginite	Ni	Ni	$P2_1/m$ or $P2_1$	a = 9.236(3) b = 12.001(6) c = 3.091(2) Å β = 90.48(7)° V = 342.6 Å ³	Nickel and Berry (1981)
Pokrovskite	Mg	Mg	$P2_1/a$	a = 12.2396(4) b = 9.3506(4) c = 3.1578(1) Å β = 96.445(5)° V = 359.12 Å ³	Perchiazzi and Merlino (2006)
Chukanovite	Fe ²⁺	Fe ²⁺	$P2_1/a$	a = 12.396(1) b = 9.407(1) c = 3.2152(3) Å β = 97.78(2)° V = 371.47 Å ³	Pekov et al. (2007)

^a Calculated here

assumed. A structural study of parádsasvárite should possibly confirm this assumption. The empirical formula (based on 5 O apfu) is $(Zn_{0.62}Cu_{0.36}Pb_{0.01})_{\Sigma 0.99}Zn_{1.00}(CO_3)(OH)_2$, with rounding errors. The end-member formula is $Zn_2(CO_3)(OH)_2$, which requires ZnO 72.40, CO₂ 19.58 and H₂O 8.02 wt.%.

Infrared spectroscopy

The IR spectrum of parádsasvárite is shown in Fig. 5. The curve is similar to that of other members of the malachite-

rosasite group reported by Frost et al. (2007a, b). Interpretation of the bands was carried out according to Frost et al. (2007a, b). The two bands observed at 661 and 738 cm⁻¹ were assigned to the ν₄ bending modes of the CO₃²⁻ ions. A band at 792 cm⁻¹ could possibly be assigned to the ν₂ bending mode of CO₃²⁻, although its intensity is rather high. The band at 993 cm⁻¹ can probably be ascribed to the δOH deformation mode. The CO₃²⁻ ν₁ band of rosasite group minerals should not be infrared active. However, because of symmetry reduction of the carbonate anion the band is observed at 1097 cm⁻¹. Two intense bands at 1379 and 1514 cm⁻¹ were attributed to ν₃ antisymmetric CO₃²⁻ stretching modes. The low intensity band at 1637 cm⁻¹ was ascribed to the water bending mode. Its appearance suggests that water molecules were adsorbed on the parádsasvárite surface. The presence of molecular water has been noted for other members of the malachite-rosasite group, i.e. for nullaginite (Nickel and Berry 1981) and for pokrovskite (Ivanov et al. 1984; Perchiazzi and Merlino 2006). In the IR spectrum of parádsasvárite two bands were observed at 3272 and 3473 cm⁻¹. These were ascribed to the stretching vibrations of hydroxyl groups. The weak, but well-separated band at 3647 cm⁻¹ could be assigned to the adsorbed H₂O, weakly hydrogen-bonded to the surface. However, it is also possible that this OH band is caused by a contamination of sub-microscopic mica-group minerals. The very weak bands between 3000 and 2800 cm⁻¹ are due to organic impurities arising from the uncompensated background of the instrument (also taking into account the very small amount of the sample investigated), although the peak at around 3000 cm⁻¹ could be a combination band.

Libowitzky (1999) gave the correlation function of O-H stretching frequencies versus O-H...O hydrogen bond lengths in the form $\nu = 3592 - 304 \times 10^9 \times \exp[-d(O\cdots O)/0.1321]$, where ν is the stretching frequency in cm⁻¹ and d(O...O) is the O...O hydrogen bond length in Å. In the structure of rosasite the two OH⁻ groups are denoted as O4 and O5. The corresponding acceptor oxygen atoms are O3 and O1 (Perchiazzi 2006). By using our determined cell parameters of parádsasvárite and the structure model of rosasite (Perchiazzi 2006), the calculated O4...O3 and O5...O1 bond lengths are 2.722 and 2.793 Å, respectively. Substituting these values into the above equation, the obtained stretching frequencies are 3250 and 3392 cm⁻¹, respectively. These wavenumbers are relative close to the measured ones, i.e. 3272 and 3473 cm⁻¹ (see Fig. 5).

Classification

Parádsasvárite is the zinc-dominant member of the malachite-rosasite group, now including nine members (Table 3), being no. 5.BA.10 in the Strunz classification (Strunz and Nickel 2001). Although Strunz and Nickel (2001) used the name

malachite group for these minerals, here the term malachite-rosasite group is preferred. This implies the existence in the group of two different, but closely related, malachite-like and rosasite-like crystal structures. As already noticed, parászasvárite is defined by zinc dominancy in both the *Me1* and *Me2* octahedrally coordinated cation sites.

May be worth now to take into account the relationships between rosasite, zincrosasite and parászasvárite. On the basis of their chemical data and of the features of their powder pattern, one can properly speak of a solid solution between rosasite, with $\text{Cu} > \text{Zn}$ in *Me1* and $\text{Zn} > \text{Cu}$ in *Me2*, and parászasvárite, with Zn dominant in both *Me1* and *Me2* sites. Regarding the zincrosasite occurrences reported in literature, both the type zincrosasite described by Strunz (1959) and the one described by Pauliš et al. (2005) can actually be referred to rosasite. The phase studied by Fehér et al. (2008) can instead be referred to parászasvárite.

Acknowledgments We thank Sándor Klaj (Pécs) for providing of the holotype sample and László Tóth (Velece) for the high quality photomicrograph of parászasvárite. We also acknowledge Philip Rawlinson (Corvinus University, Budapest) for the English text revision. Finally, the authors would like to thank the two anonymous reviewers, as well as the Associate Editor Anton Beran for their valuable comments and suggestions to improve the manuscript.

References

- Anthony JW, Bideaux RA, Bladh KW, Nichols MC (2003) Handbook of mineralogy. Vol. V: Borates, carbonates, sulfates. Mineral Data Publishing, Tucson
- Deliens M, Piret P (1980) La kolwézite, un hydroxycarbonate de cuivre et de cobalt analogue à la glaukosphaerite et à la rosasite. *Bull Minéral* 103:179–184
- Eby RK, Hawthorne FC (1993) Structural relations in copper oxysalt minerals. I. Structural hierarchy. *Acta Crystallogr B* 49:28–56
- Fehér B, Szakáll S, Bigi S (2008) Minerals of the rosasite-zincrosasite series from the Andrásy-I. mine, Rudabánya, Hungary: the zincrosasite problem [abstract]. *Mineral Spec Pap* 32:65
- Frost RL, Wain DL, Martens WN, Reddy BJ (2007a) The molecular structure of selected minerals of the rosasite group – an XRD, SEM and infrared spectroscopic study. *Polyhedron* 26:275–283
- Frost RL, Wain DL, Martens WN, Reddy BJ (2007b) Vibrational spectroscopy of selected minerals of the rosasite group. *Spectrochim Acta A* 66:1068–1074
- Holland TJB, Redfern SAT (1997) Unit cell refinement from powder diffraction data: the use of regression diagnostics. *Mineral Mag* 61:65–77
- IMA (2014) The new IMA list of minerals. Updated: March 2014. Downloaded as a pdf file from the web site <http://pubsites.uws.edu.au/ima-cnmc/> on July 21, 2014
- Ivanov OK, Malinovsky YA, Mozzherin YV (1984) Pokrovskite $\text{Mg}_2[\text{CO}_3(\text{OH})_2] \cdot 0.5\text{H}_2\text{O}$ – a new mineral from the Zlatogorskaya layered intrusive (Kazakhstan). *Zap Vses Mineral Obshch* 113:90–95 (in Russian)
- Kiss J (1960) A new ore occurrence in the environment of Nagyalya-Nagylipót-Aranybányafolyás (Mátra Mountains, NE-Hungary). *Ann Univ Sci Bp Rolando Eötvös Nomin Sect Geol* 3:55–81
- Kiss J (1964) Allitic and sillitic minerals and their role in the ore mineralization of the central part of the Mátra Mountains, N-Hungary. *Földt Közl* 94:422–431 (in Hungarian with French abstract)
- Koch S (1966) Minerals of Hungary. Akadémiai Kiadó, Budapest (in Hungarian)
- Kraus W, Nolze G (1996) Powder Cell – a program for the representation and manipulation of crystal structures and calculation of the resulting X-ray powder patterns. *J Appl Crystallogr* 29:301–303
- Libowitzky E (1999) Correlation of O-H stretching frequencies and O-H...O hydrogen bond lengths in minerals. *Monatsh Chem* 130:1047–1059
- Lovisato D (1908) Rosasite, nuovo minerale della miniera di Rosas (Sulcis, Sardegna). *Atti R Accad Lincei Cl Sci Fis Mat Nat* 17:723–728
- Mandarino J (1981) The Gladstone-Dale relationship: part IV. The compatibility concept and its application. *Can Mineral* 19:441–450
- Nickel EH, Berry LG (1981) The new mineral nullaginite and additional data on the related minerals rosasite and glaukosphaerite. *Can Mineral* 19:315–324
- Pauliš P, Novák F, Janák P (2005) Serpierite and zincrosasite from Herlíkovice near the town of Vrchlabí (Czech Republic). *Opera Corcon* 42:73–77 (in Czech with English abstract)
- Pekov IV, Perchiazzi N, Merlino S, Kalachev VN, Merlino M, Zadov AE (2007) Chukanovite, $\text{Fe}_2(\text{CO}_3)(\text{OH})_2$, a new mineral from the weathered iron meteorite Dronino. *Eur J Mineral* 19:891–898
- Perchiazzi N (2006) Crystal structure determination and Rietveld refinement of rosasite and mcguinnessite. *Z Krist Suppl* 23:505–510
- Perchiazzi N, Merlino S (2006) The malachite-rosasite group: crystal structures of glaukosphaerite and pokrovskite. *Eur J Mineral* 18:787–792
- Pouchou L, Pichoir F (1984) A new model for quantitative X-ray microanalysis. *Res Aerosp* 3:167–192
- Roberts AC, Jambor JL, Grice JD (1986) The X-ray crystallography of rosasite from Tsumeb, Namibia. *Powder Diffract* 1:56–57
- Rónai A, Pelikán P (2005) Geological map of Hungary. L-34-4 Gyöngyös, 1:100 000. Geological Institute of Hungary, Budapest (in Hungarian)
- Strunz H (1959) Tsumeb, seine Erze und Sekundärminerale, insbesondere der neu aufgeschlossenen zweiten Oxydationszone. *Fortschr Mineral* 37:87–90
- Strunz H, Nickel EH (2001) Strunz mineralogical tables, 9th edn. E. Schweizerbart'sche Verlagsbuchhandlung, Stuttgart
- Zelensky ME, Matseevsky AB, Pekov IV (2009) The computer program QSpectr for processing X-ray powder diffraction films obtained from the Debye-Scherrer camera. *Zap Ross Mineral Obshch* 138(4):103–112 (in Russian with English abstract)
- Zigan F, Joswig W, Schuster HD (1977) Verfeinerung der Struktur von Malachit, $\text{Cu}_2(\text{OH})_2\text{CO}_3$, durch Neutronenbeugung. *Z Krist* 145:412–426